5th. European Congress on
Computational Mechanics

ECCM V

11th. World Congress on
Computational Mechanics

WCCM XI

6th. European Congress on
Computational Fluid Dynamics

ECFD VI

Barcelona, Spain
July 20 – 25, 2014

Eugenio Oñate, Xavier Oliver and Antonio Huerta (Eds.)

Organized by

SEMNI

Spanish Association for Numerical
Methods in Engineering (SEMNI)
in its 25th Anniversary

with the support of
International Center for
Numerical Methods in
Engineering (CIMNE)

CIMNE

Proceedings of the jointly organized

11th. World Congress on Computational Mechanics - WCCM XI
5th. European Congress on Computational Mechanics - ECCM V
6th. European Congress on Computational Fluid Dynamics - ECFD VI
Barcelona, Spain
July 20 – 25, 2014

Edited by

Eugenio Oñate
Universitat Politècnica de Catalunya, Spain

Xavier Oliver
Universitat Politècnica de Catalunya, Spain

Antonio Huerta
Universitat Politècnica de Catalunya, Spain

11th. World Congress on Computational Mechanics (WCCM XI)
5th. European Congress on Computational Mechanics (ECCM V)
6th. European Congress on Computational Fluid Dynamics (ECFD VI)
Eugenio Oñate, Xavier Oliver and Antonio Huerta (Eds.)

A NEW STRATEGY TO SIMULATE PARTICLE CRUSHING IN DEM ANALYSIS

Matteo O. Ciantia[*], **Marcos Arroyo**[*], **Antonio Gens**[*] **and Francesco Calvetti**[†]

[*] Department of Geotechnical Engineering and Geosciences (ETCG)
Universidad Politécnica de Cataluña
Campus Norte UPC, 08034 Barcelona, Spain
e-mail: ciantia.matteo@gmail.com, www.etcg.upc.edu

[†] Dipartimento di Igegneria Civile ed Ambientale (DICA)
Politecnico di Milano
Piazza Leonardo da Vinci, 32, 20133 Milano, Italy
e.mail: francesco.calvetti@polimi.it, www.dica.polimi.it

Key Words: *DEM analysis, crushable soils, particle failure*

Abstract. The discrete element method (DEM) is progressively gaining acceptance as a modelling tool for engineering problems of direct geotechnical relevance. One area for which the method seems naturally well adapted is that of crushable soils. Grain Crushing is generally modeled using the discrete element method (DEM) via two alternative methods: replacing the breaking grains with new, smaller fragments; or by using agglomerates. The latter, despite being very helpful for the understanding of the micromechanics occurring in a single grain, becomes an unpractical tool for the modeling of larger scale problems. In fact, when considering those alternatives there is always a need to balance computational expediency, accuracy of results and soundness of principle. This work focuses on the encounter of those two last requirements, as exemplified in a series of simulation of high pressure one-dimensional and isotropic compression of Fontainebleau sand. A recently developed model for crushable soils is briefly outlined. It is shown that the upscaling procedure adopted allows a considerable reduction of computational bargain without losing accuracy in terms of grain size distribution evolution and mechanical response.

1 INTRODUCTION

To simulate crushing in soils using DEM a number of different alternatives are available: replacing the breaking grains with new, smaller fragments; or by using agglomerates. The latter, despite being very helpful for the understanding of the micromechanics occurring in a single grain [1,2], becomes an unpractical tool for the modeling of larger scale problems. Even after selecting the multigenerational, single grain approach, several modelling choices remain open. At a minimum, specification of a particle breakage criteria and a particle spawning procedure are necessary, in addition to the contact laws that are essential to DEM. A number of extra parameters emerge that require calibration in any practical application. Recently [3], the authors have proposed and tested a crushable soil DEM model that, while

biased towards effective computation, showed good ability to reproduce macroscopic responses of a variety of soils in oedometric compression. In this work, and after briefly outlining the main traits of the modeling approach selected, a new set of simulations of the one dimensional and isotropic compression of Fontainebleau sand described by [4] are presented. Particular focus is laid on the breakage model and the on the scaling formulation applied. All the numerical models described here were built using the PFC3D code [5].

2 MODEL DESCRIPTION

2.1 Particle failure criteria

The failure criteria used in the model was inspired by the works of by Russell and Wood [6,7], where the micromechanics of crushing of both single and assemblies of particles are addressed. The authors combined a two-parameter material strength criterion with the analysis of the elastic stress distribution induced by point loads on a sphere to obtain a practical failure criterion. Without entering into the details of the mathematical formulation, the end result of their analysis can be summarized as follows: a particle subject to a set of external point forces will reach failure when the maximum force acting reaches a limit condition that can be expressed as:

$$F \leq \sigma_{\lim} \pi R^2 \sin^2 \theta_0 = \sigma_{\lim} A_F \tag{1}$$

where $\sigma_{\lim}$ is the limit strength of the material, R is the particle radius and θ_0 is half of the solid angle "seen" from the center of the particle which defines the small area of stress application, A_F. As indicated in (1), the limiting force is obtained as the product of a limit strength value, $\sigma_{\lim}$, dependent on material parameters, and a contact area A_F. The latter may be taken as a constant, making θ_0 a model parameter as in [8], or may be considered as the actual contact area between two stressed particles, and hence dependent on both contact law and contact force (see [3]). In this work the contact solid angle is taken as the result Hertzian contact theory mechanics. For smooth spheres the radius of the contact area is:

$$r_H = \left(\frac{3Fr'}{4E'} \right)^{1/3} \tag{2}$$

where

$$r' = \left(\frac{1}{r_1} + \frac{1}{r_2} \right)^{-1} \tag{3}$$

$$E' = \left(\frac{1-v_1^2}{E_1} + \frac{1-v_2^2}{E_2} \right)^{-1} \tag{4}$$

where r_1 and r_2 are the radius of the contacting spheres and E_i v_i their moduli. Hence, if Hertzian contact theory is used to calculate the evolution of contact area, the limit force reads:

$$F_{\lim} = \left[\sigma_{\lim} \pi \left(\frac{3r'}{4E'} \right)^{2/3} \right]^3 \tag{5}$$

To incorporate within-size variability into the simulation, the limit strength, σ_{lim}, is assumed to be normally distributed, with a mean value indicated as σ_{lim0}, for a given sphere size. In addition, a size effect correction is incorporated as a dependency of the mean strength value on particle diameter, casted in a Weibull-like form:

$$\sigma_{lim} = \sigma_{lim,0} \left(\frac{d}{d_0} \right)^{-3/m} \tag{6}$$

The limit condition hence reads:

$$F \leq \left[\sigma_{lim,0} \left(\frac{d}{d_0} \right)^{-3/m} \pi \left(\frac{3r'}{4E'} \right)^{2/3} \right]^3 \tag{7}$$

2.2 Particle splitting configuration

Once the limit condition is reached, a particle, modeled with a sphere in PFC, will split into smaller inscribed tangent spheres.
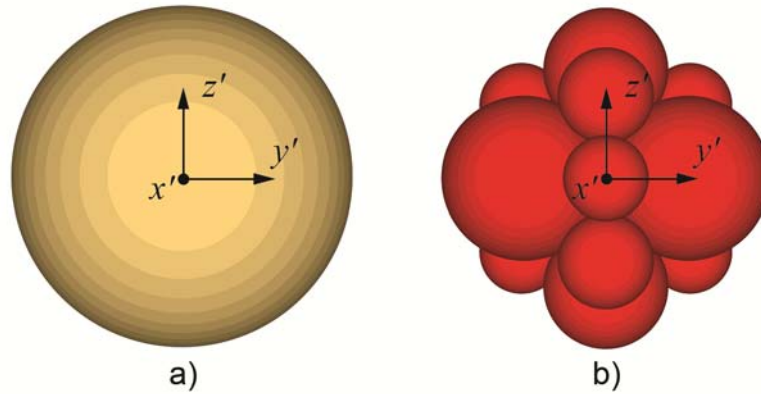

Figure 1: a) Initial particle, b) Particle splitting configuration

It is clear that this way of modeling crushing does not conserve the mass within the numerical simulation. This is acceptable if the mass lost is cosntituted by finer particles that have a small influence on the macroscopic mechanical response. Indeed, smaller particles do have a lesser role than large ones on force transmission through a granular mass [9],[10]. On the other hand, the mass lost is always accounted when calculating for instance, porosity, n, or the evolution of grain size distribution (GSD) with time. For the latter, the deleted mass is assumed to have a fractal distribution with a maximum particle size smaller that the smallest particle produced during the crushing event. Ciantia et al in [3] describe this procedure and compare alternative splitting configurations, concluding that the 14-ball crushed configuration (47% volume of mother particle is removed in each crushing event) represented in Figure 1 is accurate enough for macroscopic behavior. The daughter fragments adopt the velocity and material parameters of the mother particle except for the intrinsic strength (σ_{lim0}) that is randomly assigned in accordance with the assumed normal distribution criteria.

2.3 Contact law

In this work the contact law is the simplified Hertz-Mindlin law, and the standard formulation ([5]) is used. The normal and shear stiffness are calculated as:

$$k_N = \left(\frac{2\langle G \rangle \sqrt{2\dfrac{D_1 D_2}{D_1 + D_2}}}{3(1 - \langle v \rangle)} \right) \sqrt{U} \tag{8}$$

$$k_S = \left(\frac{2\left(\langle G \rangle^2 \, 3(1 - \langle v \rangle) \dfrac{D_1 D_2}{D_1 + D_2} \right)^{1/3}}{2 - \langle v \rangle} \right) |F|^{1/3} \tag{9}$$

where U is the sphere overlap, F is the magnitude of the normal contact force and the $\langle \ \rangle$ brackets indicate the mean value of the quantity considered of the two balls in contact (shear modulus G and Poisson ratio v).

2.4 Upscaling procedure

In this section the aim is to show how a simple upscaling procedure can be used to simulate the same problem using a smaller number of particles. The idea is to scale the particle size maintaining constant other geometrical dimensions of the problem (Figure 2). In this way, as the particle size increases their number decreases. The upscaling procedure is judged successful if the macroscopic quantities of interest such as compressibility, yield stress in normal compression lines and so on, remain unchanged. Also the grading evolution computed during compression should be correct when scaled back.
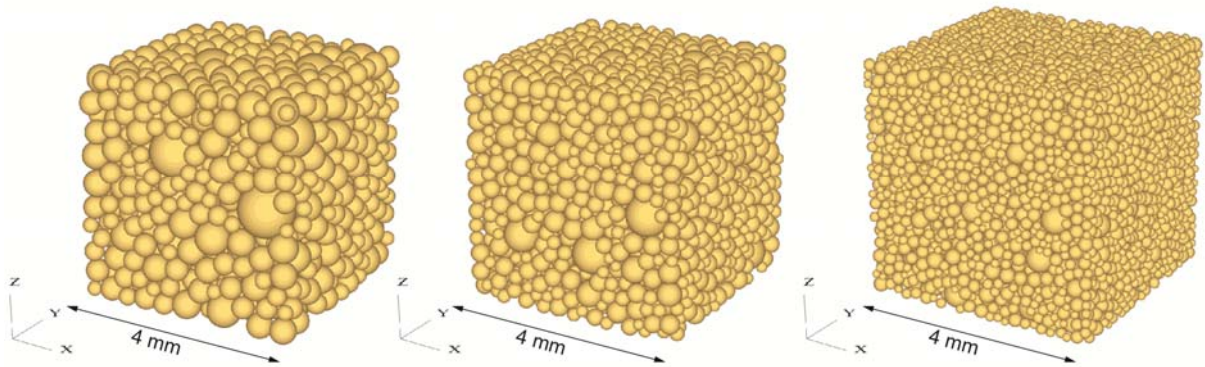

Figure 2: Scale factor = 2 (left) corresponding to 1304 particles, scale factor = 1.5 (center) corresponding to 3084 particles, and scale factor = 1 (right) corresponding to 10397 particles for the same numerical tests.

Regarding particle stiffness, the simplified Hertz-Mindlin, the standard formulation ([5]) already includes a scaling factor when calculating the normal and shear contact stiffness (see eqs. (8) and (9)). On the other hand, scaling of particle strength is made simple by the fact that

a reference dimension is already present in the formulation of the size dependency factor in equation (7). The scale factor is then just factored in the definition of the reference dimension d_0. Therefore:

$$F \leq \left[\sigma_{\lim,0} \left(\frac{d}{\mathrm{N}d_0} \right)^{-3/m} \pi \left(\frac{3r'}{4E'} \right)^{2/3} \right]^3 \tag{10}$$

where N represents the scaling factor. Uniform scaling of particle size shifts the GSD line towards the right proportionally to the scaling factor N. In order to compare GSD evolutions of the same test with different scaling factors all GSD are divided by the scale factor N (downscaling procedure).

3   MODEL CALIBRATION

The reference material is the Fontainebleau Sand employed by [4]. A cubic numerical specimen, with a side length of 4 mm is filled with about 10000 non-scaled randomly assembled weightless rigid particles of different sizes (following the grain size distribution of Fontainebleau Sand). The boundaries of the cubic specimens are defined by introducing smooth "wall" elements, to which either stress (through applied forces) or displacement rates (through prescribed wall speed) can be imposed. The contact law parameters (contact friction angle ϕ, shear modulus G and Poisson ratio v) are calibrated simulating low confining pressure drained triaxial compression of a dense and loose sample of Fontainebleau sand by [11] while the particle failure criteria parameters (mean particle strength $\sigma_{\lim 0}$ and its coefficient of variation CV for a given sphere size and the Weibull modulus m) are calibrated simulating the one dimensional compression test from [4].
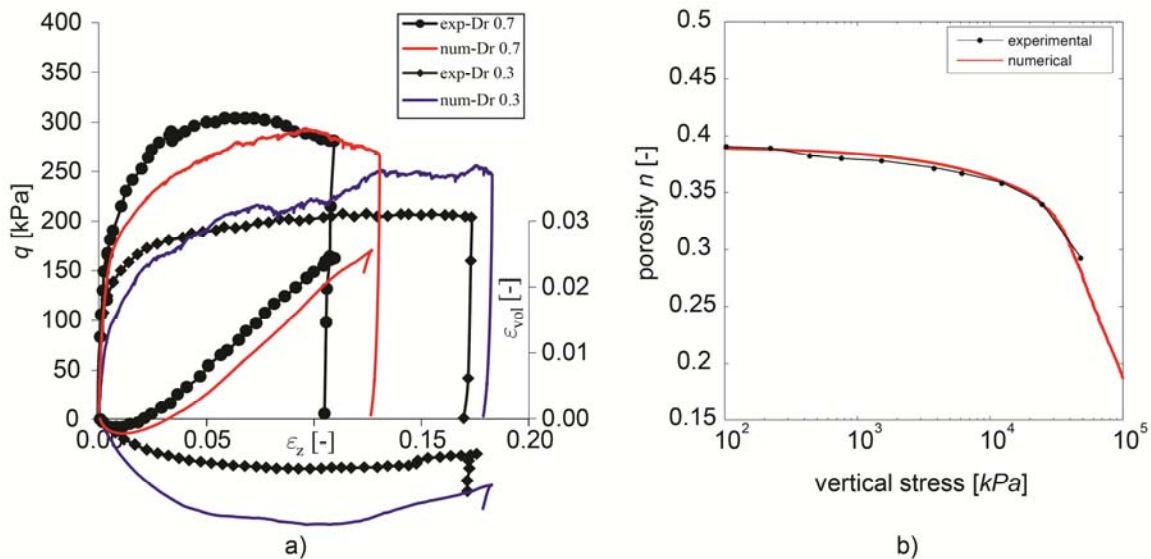

Figure 3 DEM-simulation of a) drained triaxial compression test (cell pressure 100 kPa) deviatoric stress vs axial strain and volumetric strain vs axial strain and b) oedometric compression and of Fontainebleau sand.

In Figure 3 the numerical simulations used to calibrate the contact and crushing parameters

1276

are depicted and the corresponding calibrated model parameters are summarized in Table 1. In the next section the upscaling procedure is investigated in terms of effectiveness and efficiency.

Table 1 Discrete-element method input parameters for simulation

d_{50} [mm]	ϕ [rad]	G [kPa]	ν [–]	$\sigma_{lim,0}$ [kPa]	CV	m	d_0 [mm]
0.21	0.27	3e6	0.3	5e6	1	10	2

4 NUMERICAL SIMULATIONS

4.1 Effectiveness of the upscaling procedure

In this section, simulations of one dimensional and isotropic compression tests of three numerical samples characterized by a different scaling factor are presented. For this purpose, two other numerical samples, characterized by a scale factor of 1.5 and 2 respectively are also generated. The initial dense packing of the three samples characterized by the same porosity (n=0.39) are reported in Figure 2. The simulation set is fully described in Table 2. The ID of the numerical simulations (Test-ID) employed in later figures is composed by one letter and one number respectively. The letters identify the type of test simulated (O stands for one dimensional compression and I stands for the isotropic; the numbers indicate the scaling factor. The numerical tests took place under load control.

Table 2 Initial conditions of the three numerical samples

Test ID	Stress path	scale factor N	Initial number of particles N_i	Control type	Load rate, L_R	Top wall velocity, Wv [m/s]	Local damping
O-2	oedometric	2	1304	Load	0.1	-	0.05
O-1.5	oedometric	1.5	3084	Load	0.1	-	0.05
O-1	oedometric	1	10397	Load	0.1	-	0.05
I-2	isotropic	2	1304	Load	0.1	-	0.05
I-1.5	isotropic	1.5	3084	Load	0.1	-	0.05
I-1	isotropic	1	10397	Load	0.1	-	0.05

As described in [3] the rate of load increase is chosen so that the mechanical response does not change if this value is further decreased. In other words it is the maximum load rate compatible with quasi-static conditions. As the vertical stress during the simulation covers several orders of magnitude the following expression controlling the load increment is used:

$$\sigma_j^{i+1} = \sigma_j^i + L_R \left[\sigma_{ref} + \log\left(\frac{\sigma_j^i}{\sigma_{ref}} \right) \right] \qquad (11)$$
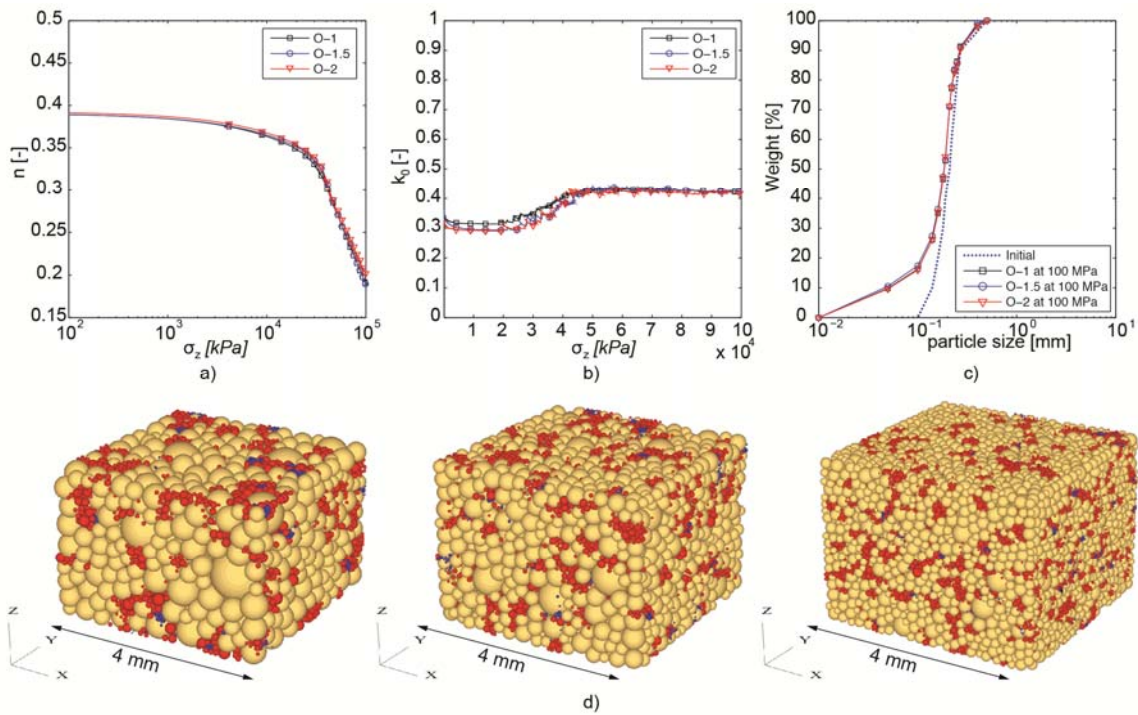
Figure 4 DEM-simulation of one dimensiona compression: a) n-vertical stress b) k_0-vertical stress c) grain size distribution at 100 MPa for the three numerical samples and d) scale 2, 1.5 and 1 samples at 100 MPa
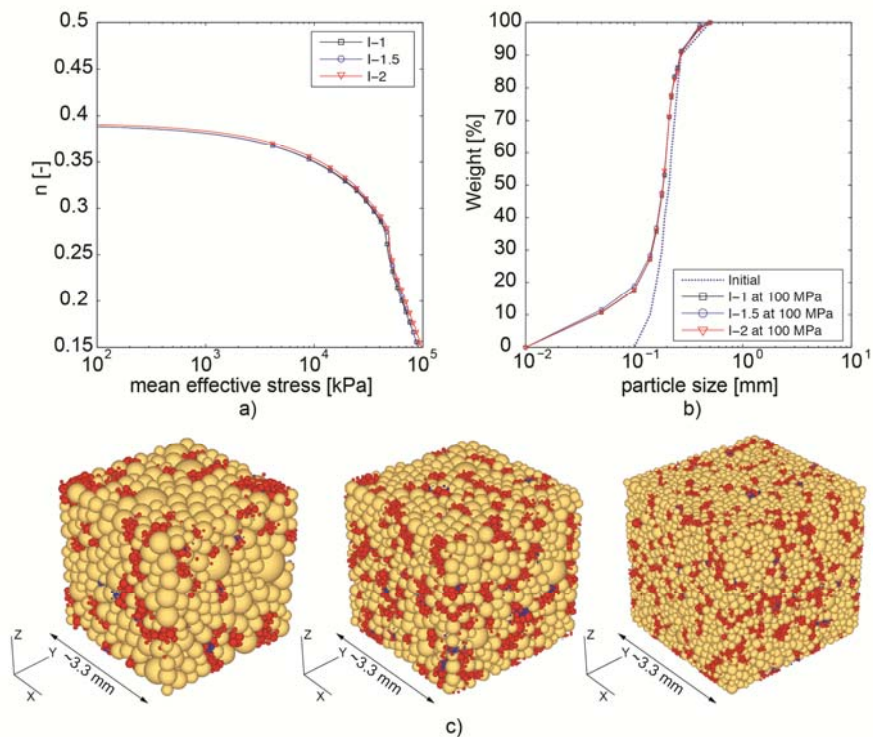

Figure 5 DEM-simulation of isotropic compression: a) n-mean effective stress, b) grain size distribution at 100 MPa of vertical stress for the three numerical samples and c) scale 2, 1.5 and 1 samples at 100 MPa

where L_R is the load rate, i indicates the step of the calculation and σ_{ref} is a reference stress of 1 kPa. The numerical simulations of the one dimensional compression test are compared in Figure 4 while simulations concerning the isotropic compression tests are displayed in Figure 5. The results show that the upscaling procedure allows to reproduce effectively both the mechanical and grain size distribution evolution. Finally in Figure 6 the stress paths are plotted in the deviatioric plane, q-p'. In Figure 6c the grading index I_G, expressed by the area ratio of the current grading to the limiting grading (see Figure 6a), is represented as a function of mean effective stress. Initially, I_G is equal to about 0.735 and, as the GSD , it increases along the loading path. The good match between the curves indicates that the upscaling procedure is also effective for the description of the grading index evolution.
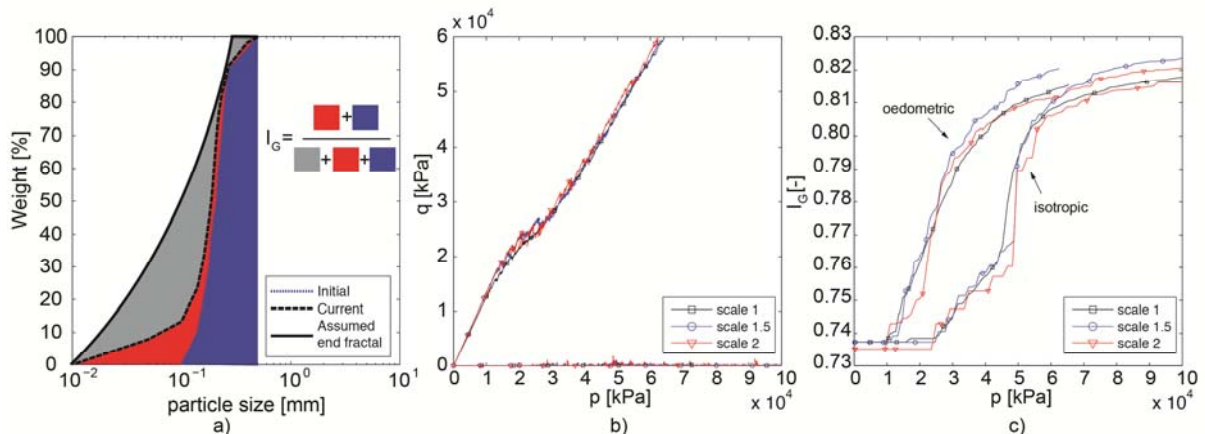

Figure 6 isotropic and one dimensional compressio stress paths with corresponding IG index evolution for a-b) scale 1, c-d) scale 1.5 and e-f) scale 2.

4.2 Efficiency of the upscaling procedure

In the previous section we have highlighted the performance of the model from the point of view its ability to reproduce the experimental observations and the soundness of the upscaling procedure was also addressed. However, if the final goal is to apply the calibrated discrete materials to simulate larger scale problems, it is also pertinent to discuss model efficiency. In this context efficiency it is closely represented by model runtime, since all the simulations were performed using the same hardware (Intel® Core™ i7-3770 CPU @ 3.40 GHz with 8.00 GB of RAM). Table 3 thus summarizes several outcomes of the model: model runtime, initial and final particle number and crush events. Figure 7 represents the effect on simulation runtime of initial number of particles. As expected, a major factor affecting model efficiency seems to be the number of particles at the beginning of the simulation. Since this number scales with the cube of the linear scaling factor, doubling the scaling factor results in runs that are typically around 6 times faster. This clearly implies that the choice of the particle spawning procedure has a very important bearing on the computational efficiency of the model. The compounded effect of scaling particle size and limiting spawning fragments in these simulations is a factor close to 100 in simulation runtime.

Table 3 Discrete-element method model results

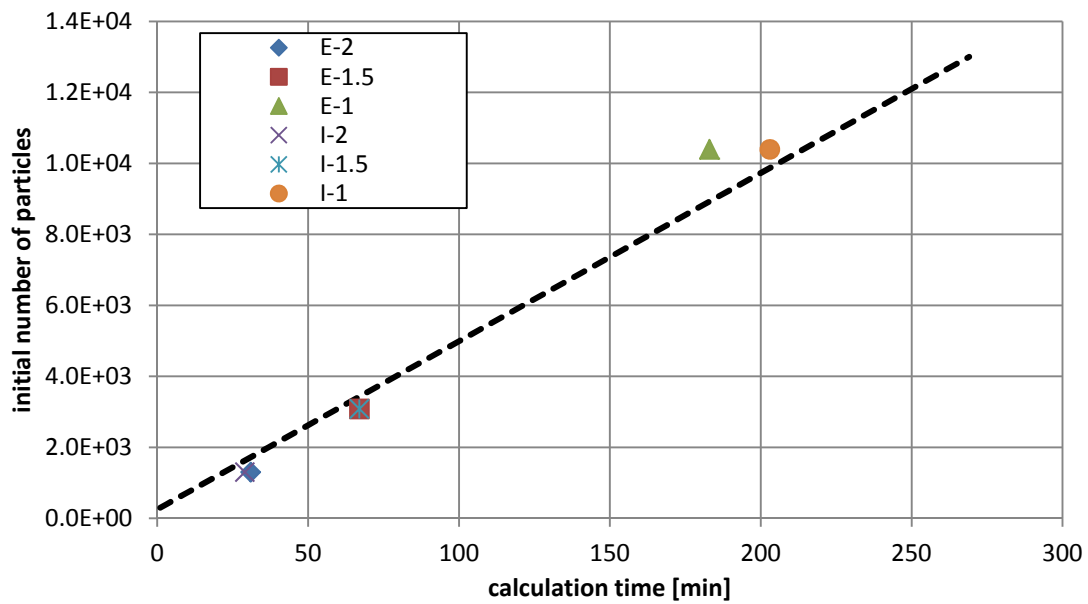| Test ID	N	L_R	Wv [m/s]	N_i	N_e	Cruhing events	Model run [min]
E-2	2	0.1	-	1304	4372	236	31
E-1.5	1.5	0.1	-	3084	9974	530	67
E-1	1	0.1	-	10397	37658	2097	183
I-2	2	0.1	-	1304	5230	302	29
I-1.5	1.5	0.1	-	3084	10819	595	67
I-1	1	0.1	-	10397	40778	2337	203

Figure 7 Simulation time vs initial number of particles.

5   CONCLUSIONS

A multigenerational discrete element method approach has been used to simulate one-dimensional and isotropic compression of Fontainebleau sand. The spawning procedure advocated results in lost mass during the simulation; however that loss does not seem to affect significantly the ability of the models to match the experimentally observed macroscopic response. This model feature takes advantage of the highly redundant and skewed mechanics of force transmission through discrete materials. This work also substantiates the computational efficiency of the upscaling rules proposed. It is shown that calculation time can be reduced considerably with little difference in terms of mechanical behavior and GSD evolution. The proposed procedure can be considered as a springboard for future large-scale simulations or as a numerical tool to support continuum-based constitutive models (for example see [12]).

1280

REFERENCES

[1] Y.P. Cheng, Y. Nakata, and M.D. Bolton, Discrete element simulation of crushable soil. *Géotechnique* Vol. **53**, No. 7, pp. 633–641, 2003.

[2] M.D. Bolton, Y. Nakata and Y.P. Cheng, Micro- and macro-mechanical behaviour of DEM crushable materials. *Géotechnique*, Vol. **58**, No. 6, pp. 471–480, 2008.

[3] M. Ciantia, M. Arroyo, F. Calvetti and A. Gens, An efficient approach for DEM modelling of crushing in soils. *Géotechnique* submitted for publication, 2014

[4] Yang, Z. X., Jardine, R. J., Zhu, B. T., Foray, P. & Tshua, H. C. (2010) Sand grain crushing and interface shearing during displacement pile installation in sand *Géotechnique* 60, No. 6, 469–482

[5] Itasca (2008). Particle flow code in three dimensions: Software manual. Minnesota, MN, USA

[6] A.R. Russell and D. Muir Wood, Point load tests and strength measurements for brittle spheres. I. *J. of Rock Mech. And Mining Sciences* Vol. **46**, pp. 272–280, 2009.

[7] A.R. Russell, D.Muir Wood and M. Kikumoto, Crushing of particles in idealised granular assemblies. *J. Mech. Phys. Solids*, Vol. **57**, No. 8, pp. 1293–1313, 2009.

[8] M. Ciantia, M. Arroyo, F. Calvetti and A. Gens, Particle failure in DEM models of crushable soil response. *NUMGE*, 2014

[9] Minh, N. H. & Cheng, Y. P. (2013). A DEM investigation of the effect of particle-size distribution on one-dimensional compression, Géotechnique 63, No. 1, 44–53

[10] Esnault, V. P. B., & Roux, J. N. (2013). 3D numerical simula-tion study of quasistatic grinding process on a model granu-lar material. Mechanics of Materials, 66, 88-109

[11] Seif El Dine, B., Dupla, J. C., Frank, R., Canou, J. & Kazan, Y. (2010) Mechanical characterization of matrix coarse-grained soils with a large-sized triaxial device. Can. Geotech. J. 47: 425–438

[12] M. Ciantia, M. Arroyo, F. Calvetti and A. Gens, A numerical investigation of the incremental behavior of crushable granular soils. *Géotechnique Letters* submitted for publication, 2014